JACS
JOURNAL OF THE AMERICAN CHEMICAL SOCIETY

ARTICLE

pubs.acs.org/JACS

Real-Time Measurements of Protein Dynamics Using Fluorescence Activation-Coupled Protein Labeling Method

Toru Komatsu,[†,⊥] Kai Johnsson,[§] Hiroyuki Okuno,[‡,⊥] Haruhiko Bito,[‡,⊥] Takanari Inoue,[∥] Tetsuo Nagano,[†,⊥] and Yasuteru Urano*[,†,‡]

[†]Graduate School of Pharmaceutical Sciences and [‡]Graduate School of Medicine, The University of Tokyo, 7-3-1, Hongo, Bunkyo-ku, Tokyo, 113-0033, Japan

[§]Institut des Sciences et Ingénierie Chimiques, Ecole Polytechnique Fédérale de Lausanne, CH-1015, Lausanne, Switzerland

[∥]Department of Cell Biology, Center for Cell Dynamics, School of Medicine, Johns Hopkins University, Baltimore, Maryland 21205, United States

[⊥]JST CREST, Sanbancho-bldg., 5 Sanbancho, Chiyoda-ku, Tokyo, 102-0075, Japan

Supporting Information

ABSTRACT: We present a fluorescence activation-coupled protein labeling (FAPL) method, which employs small-molecular probes that exhibit almost no basal fluorescence but acquire strong fluorescence upon covalent binding to tag-proteins. This method enables real-time imaging of protein labeling without any washout process and is uniquely suitable for real-time imaging of protein dynamics on the cell surface. We applied this method to address the spatiotemporal dynamics of the EGF receptor during cell migration.

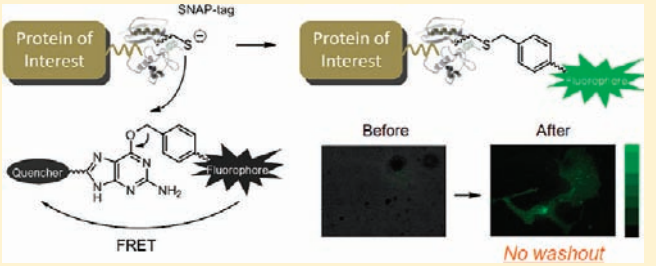

INTRODUCTION

Understanding protein dynamics is critical to decipher the role of proteins in specific cellular events that underlie sophisticated living systems. Detection and visualization of protein movements, in particular, has great potential to uncover dynamic protein functions.[1] To this end, expression of genetically encoded fusion proteins tagged with fluorescent proteins (FPs) and, more recently, novel chemistry-based strategies to label and monitor specific tag-proteins have proved powerful.[2−5] For example, FlAsH,[2] which binds to a tetracysteine motif, and O^6-benzylguanine (BG) derivatives,[6] which form a covalent bond with a tag-protein, O^6-alkylguanine-DNA-alkyltransferase (SNAP-tag), are frequently used in protein visualization experiments. A major advantage of such small molecule-based labeling is the enormous potential for adjusting the functions of the probes as required by means of chemical modification.[3,7−9] A major added value is that one can precisely control the location[10,11] and timing[12] of labeling by appropriate regulation of probe delivery. For example, selective visualization of a cell-surface pool of proteins can be achieved by bath application of membrane-impermeable protein labeling probes.[10] However, there remains one major caveat associated with all currently available protein labeling techniques, namely, the inability to directly detect labeled protein during the labeling reaction, which occurs in the presence of an excess of unreacted or nonspecifically bound probe. For that reason, an extensive washout procedure to remove excess unlabeled probe is a prerequisite for protein visualization and quantification, thus rendering impossible continuous monitoring of the dynamics of a specific pool of proteins. To overcome this generic problem, we have developed a novel fluorescence activation-coupled protein labeling (FAPL) probe based on the SNAP-tag labeling system. A small-molecular probe was designed so that its fluorescence is dramatically activated (affording an extremely high signal-to-noise ratio) concomitantly with selective labeling of a tag-protein. Such properties have been recognized as desirable since the first development of protein labeling probes[2,13,14] but have not been attained in current systems, for which a washout process remains essential due to lack of specificity or incomplete fluorescence quenching. For example, a protein labeling probe that showed fluorescence activation upon labeling of SNAP-tag protein has been reported,[15] but the fluorescence activation, which was based on guanine-based quenching, was as low as 30-fold and the background fluorescence was not negligible. Here, we have developed FAPL probes for the SNAP-tag protein based on the Förster resonance energy transfer (FRET)[13,16] principle (Figure 1a). The design concept has been used to obtain probes for visualization of physiological protease activities,[17] but our aim here was to achieve a sufficiently high reaction rate, high fluorescence activation ratio, as well as high specificity toward a generally used tag-protein without physiological functions.

Received: January 10, 2011
Published: April 07, 2011

dx.doi.org/10.1021/ja200225m | J. Am. Chem. Soc. 2011, 133, 6745–6751

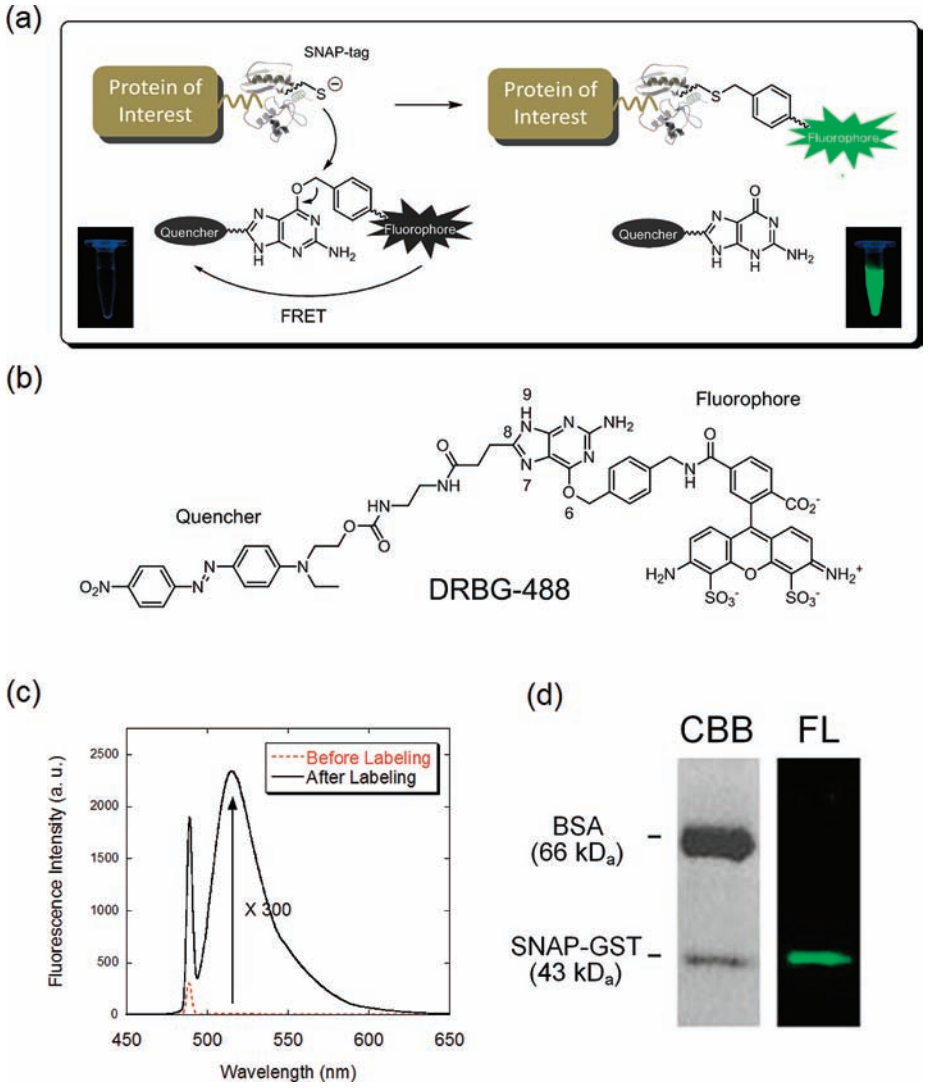

Figure 1. (a) Design of fluorescently activatable SNAP-tag labeling probe. Images of solution before (left) and after (right) labeling under excitation with a UV lamp (365 nm) are shown. (b) Chemical structure of DRBG-488. (c) Fluorescence spectra of DRBG-488 (1 μM) in phosphate buffer (100 mM, pH 7.4) before and after addition of SNAP-GST (1.5 μM). (d) The result of CBB staining and fluorometric analysis of the SDS-PAGE gel of SNAP-GST (43 kDa, 0.5 μM) and BSA (66 kDa, 2 μM) incubated with DRBG-488 (2 μM) for 90 min.

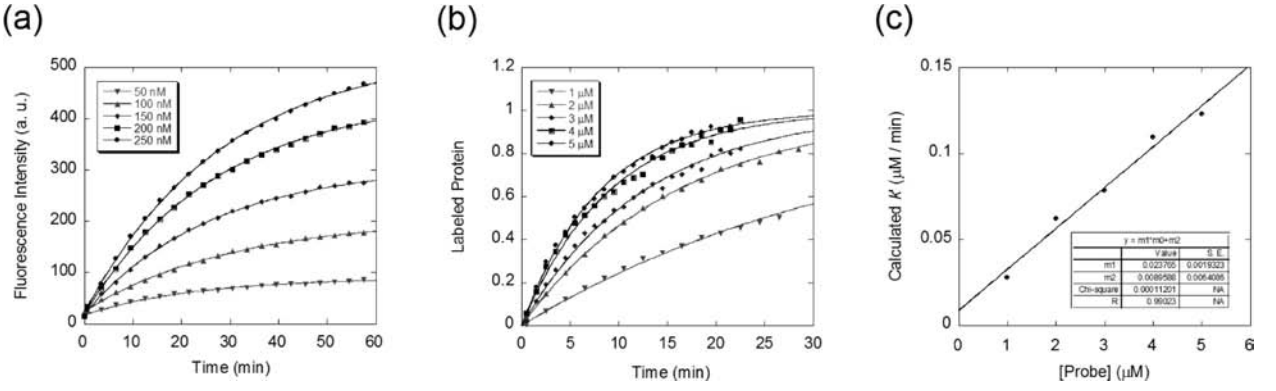

Figure 2. Kinetic study of SNAP-tag labeling with DRBG-488. (a) Fluorescence increase of DRBG-488 (2 μM) in labeling of SNAP-tag at various protein concentrations (50−250 nM). (b) Fluorescence increase of DRBG-488 (1−5 μM) in labeling of SNAP-tag (50 nM). (c) Plot of probe concentration versus calculated k' (= k[S]), showing a linear relationship.

By careful design, we have developed FAPL probes that meet these criteria, allowing practical labeling of general-tag protein in real-time without any washout. We confirmed that these probes are versatile research tools to study protein dynamics.

dx.doi.org/10.1021/ja200225m |J. Am. Chem. Soc. 2011, 133, 6745–6751

RESULTS AND DISCUSSION

The SNAP-tag forms a covalent bond with BG derivatives by nucleophilic attack at the active site cysteine, resulting in release of the guanine moiety.[6] In designing our probes, we had to decide which position of the guanine moiety would be most suitable for attachment of the fluorescence quencher, so we examined the structure−activity relationship in the labeling reaction. Crystallographic studies of O^6-benzylguanine-bound SNAP-tag protein have shown that the N-1, N-3, N-7, and O-6 positions of O^6-alkylguanine should be preserved for substrate recognition of the enzyme.[6,18,19] Therefore we compared the reaction rates of C-8 and N-9 modified O^6-benzylguanine derivatives and found that modification at the C-8 position was superior from the viewpoint of fast labeling of SNAP-tag (Figure S1 and S2 in the Supporting Information). On the basis of this result, we designed and synthesized a fluorescently activatable SNAP-tag labeling probe in which the fluorophore is modified at the benzyl moiety and the quencher is modified at the guanine moiety via a linker attached at the C-8 position. The synthesis was done via a fully protected benzylguanine scaffold with appropriate linkers for fluorophores and quenchers. From this synthetic intermediate, one can modify the components in the order of quencher motif to fluorophore motif (Scheme S1 in the Supporting Information) or vice versa (Scheme S2 in the Supporting Information). Both synthetic routes gave similar yields in this case. Here, we selected disperse red-1 as a quencher and chose two fluorophores, Alexafluor-488 and fluorescein, to synthesize probes named DRBG-488 and DRBGFL, respectively (Figure 1b). Both fluorophores show fluorescence at similar wavelengths (around 500 nm), but the design goals are different in terms of probe delivery. In the former probe, Alexafluor-488 has multiple negative charges which render the probe completely membrane-impermeable,[9] while in the latter, fluorescein can be modified with diacetyl protection (DRBGFL-DA) to obtain a cell-permeable probe.[6] Both DRBG-488 and DRBGFL showed almost no fluorescence, demonstrating high FRET efficiency (>99%), and were completely stable in the absence of SNAP-tag protein. However, after SNAP-tag protein was labeled, fluorescence rapidly appeared, with a fluorescence activation ratio of over 300 (Figure 1c and Figure S4 in the Supporting Information). We observed no background labeling of excess amounts of other proteins in the system, confirming that the labeling and fluorescence activation were completely selective for SNAP-tag protein (Figure 1d). The labeling reaction of DRBG-488 proceeds via pseudofirst order kinetics, and the time required to achieve 50% labeling of protein ($\tau_{1/2}$) was calculated to be about 6 min when we used 5 μM DRBG-488 (Figure 2). Among protein labeling probes that have so far been reported to achieve fluorescence activation,[2,13,14] this labeling system is far superior in speed and selectivity of labeling as well as in the ratio of fluorescence activation and is therefore expected to offer great advantages in practical use.

To establish the utility of these probes for live cell imaging, we applied DRBG-488 and DRBGFL-DA to label and visualize SNAP-tag expressed on the cell surface or in cytosol, respectively. As a model extracellular SNAP-tag protein, we prepared a SNAP-tagged EGF receptor, named (N) SNAP-EGFR, in which SNAP-tag protein was inserted after the signal sequence, resulting in a N-terminal SNAP-fusion of the mature EGF receptor.[20] The EGF receptor is a cell-surface tyrosine-kinase receptor for growth factors such as EGF and transforming growth factor (TGF)-α and has well-established roles in proliferation, differentiation, and migration of both normal and tumor cells.[21−24] We therefore sought to scrutinize the relationship between its dynamics and biological functions.

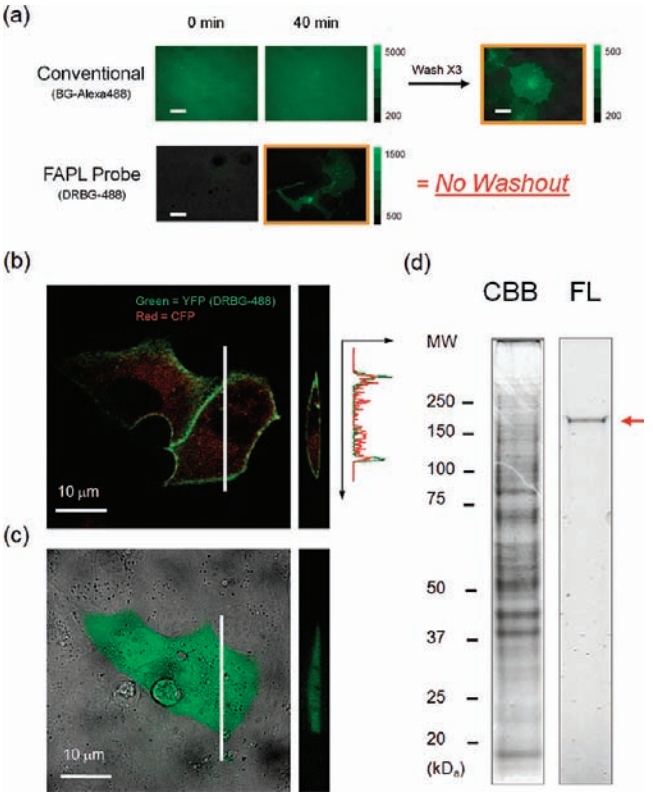

Figure 3. (a) Comparison of FAPL probe (DRBG-488, bottom) and conventional protein labeling probe (BG-Alexa488, top). (N) SNAP-EGFR-expressing COS7 cells were incubated with conventional protein labeling probe BG-Alexa488 (1 μM) or FAPL probe DRBG-488 (2 μM). For BG-Alexa488, cells were washed with PBS three times before fluorescence images were taken. The quantitative fluorescence values are summarized in Figure S6 in the Supporting Information. (b) Overlay of confocal fluorescence images of MDCK cells expressing SNAP-EGFR-CFP after 1 h of labeling with DRBG-488 (2 μM). Green = YFP channel (DRBG-488), red = CFP channel (ECFP). A vertically scanned fluorescence image taken at the position indicated by the white line is also shown, along with a line graph of fluorescence intensity. (c) Overlay of confocal fluorescence and DIC images of MDCK cells expressing cytosolic SNAP-tag after 3 h of labeling with DRBGFL-DA. A vertically scanned fluorescence image taken at the position indicated by the white line is also shown. (d) CBB-staining and fluorescence images of cell lysate from (N) SNAP-EGFR-expressing cells labeled with DRBG-488. A red arrow indicates the expected molecular weight of (N) SNAP-EGFR.

We first confirmed that incubation with cell-impermeable DRBG-488 allowed immediate visualization of (N) SNAP-EGFR without any washout process (Figure 3a and Figure S5 and Supplementary Movie 1 in the Supporting Information). This is in sharp contrast with conventional protein labeling with a nonactivatable dye (BG-Alexa488), for which a lengthy post-incubation washout period was required before effective visualization was possible. The labeling reaction was completely selective for SNAP-tagged EGF receptor (Figure 3d) and occurred specifically on the cell surface (Figure 3b and Figure S7 in the Supporting Information). Immunofluorescence staining indicated that our method could visualize SNAP-tagged EGF receptor expressed at a level comparable to that of physiological

dx.doi.org/10.1021/ja200225m |J. Am. Chem. Soc. 2011, 133, 6745–6751

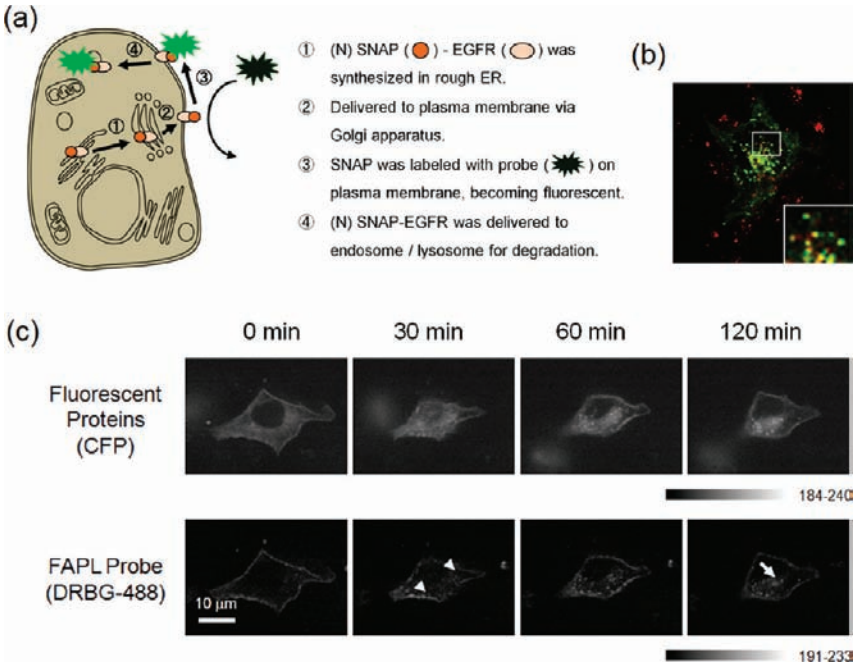

Figure 4. (a) The concept of a membrane trafficking study with use of FAPL probes. (b) The costaining image of (N) SNAP-EGFR-expressing COS7 cells labeled with DRBG-488 (2 μM, green) and lysosome marker, lysotracker (50 nM, red), in the presence of EGF (100 nM). (c) Confocal fluorescence images of SNAP-EGFR-CFP-expressing MDCK cells labeled with DRBG-488 (2 μM) for 2 h. Fluorescence images at CFP channel (top, ECFP) and YFP channel (bottom, DRBG-488) are shown. EGF (100 ng/mL) was added at 5 min, and fluorescence images were taken every 1 min. Formation of small vesicles right after EGF stimulation (white arrowhead) and accumulation to lysosomes (arrow) were more clearly visualized in FAPL-based imaging. See Supplementary Movie 2 in the Supporting Information for details.

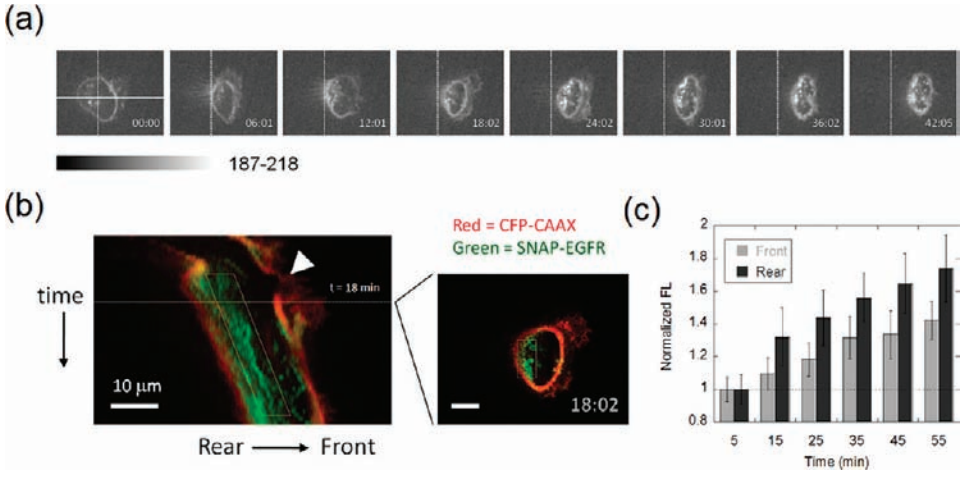

Figure 5. Application of FAPL probe for cell migration study. (a) Fluorescence images of SNAP-EGFR (labeled with DRBG-488) during MDCK cell migration induced by uniform EGF stimulation. Vertical line (dotted) represents the start position of migration, and horizontal line represents the axis on which kymograph analysis in part b was performed. See Supplementary Movie 3 in the Supporting Information for details. (b) The result of kymograph analysis of SNAP-EGFR (green) and membrane marker CFP-CAAX (red). Internalization of SNAP-EGFR was observed during cell migration, mainly from the rear of the cell (dotted parallelogram). Ruffle formation was also observed during 10−30 min (white arrowhead). One representative image is shown as an overlay of SNAP-EGFR (green) and CFP-CAAX (red) fluorescence (t = 18 min). (c) Fluorescence intensities of newly formed SNAP-EGFR vesicles at the front and rear of cells, with respect to direction of motion. On the kymograph, the region of interest (ROI, 2.5 mm × 10 min) for measurement of fluorescence intensities was set inside cells adjacent to the membrane at the front and rear of cells. Fluorescence intensities were normalized to the average fluorescence intensity at 0−10 min. Repeated-measures ANOVA showed a significant difference between the rear and front sides (∗, $P < 0.05$). Data are averages of 10 cells that showed typical migration. Error bar represents the standard error (SE).

EGF receptor (Figure S6 in the Supporting Information). We confirmed that labeling occurred with pseudofirst order kinetics, just as in the *in vitro* experiments, and the calculated kinetic constant was about half of that in the *in vitro* experiments (Figures S8 and S9 in the Supporting Information). We assume this difference might arise from the structural difference of

dx.doi.org/10.1021/ja200225m |*J. Am. Chem. Soc.* 2011, 133, 6745–6751

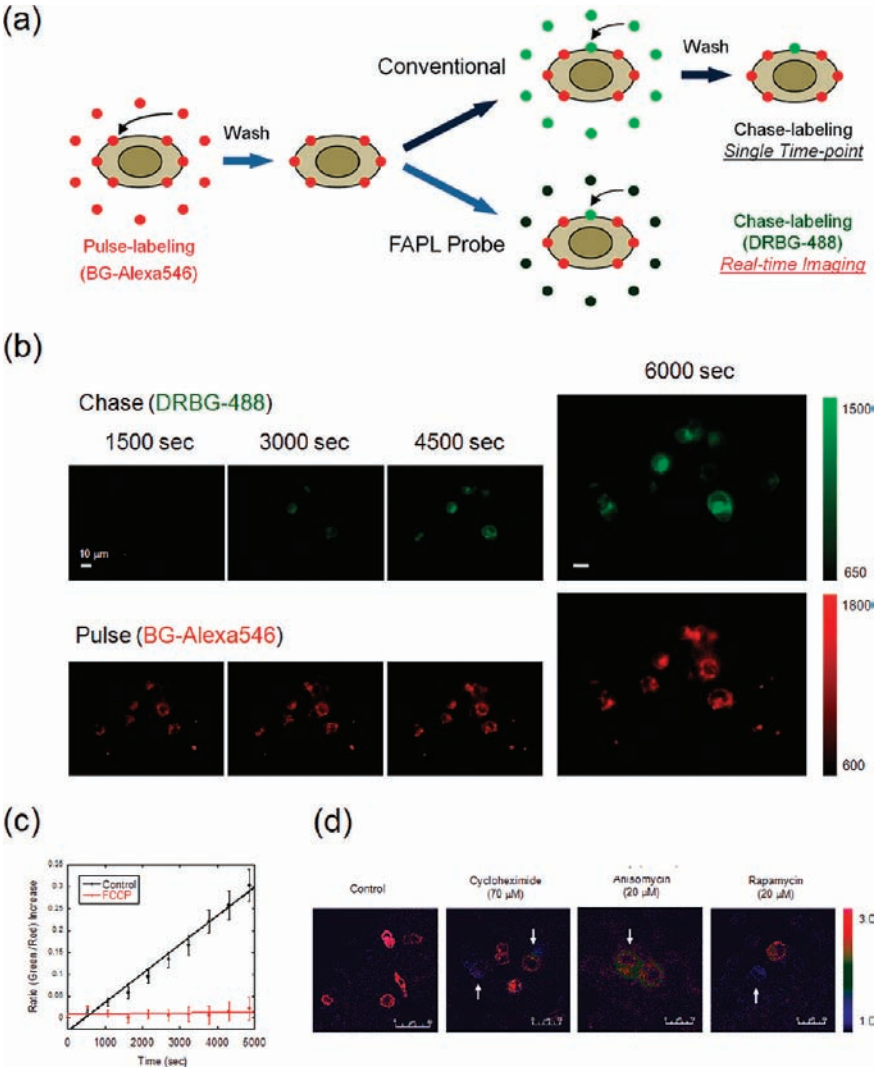

Figure 6. (a) A schematic view of real-time pulse-chase labeling to monitor protein newly delivered to the cell surface. (b) The result of real-time pulse (BG-Alexa546)-chase (DRBG-488) labeling of (N) SNAP-EGFR-expressing HEK293 cells. (c) Fluorescence ratio (green/red) increase of control cells (black) and ATP-starved (red) cells in real time pulse-chase labeling. Error bar represents SE (n = 5 for the control and n = 3 for FCCP-treated cells). (d) The result of pulse-chase labeling of HEK293 cells pretreated and coincubated with protein synthesis inhibitors. Pulse-chase labeling was performed with pretreatment (90 min) and coincubation with cycloheximide (70 μM), anisomycin (20 μM), or rapamycin (20 μM). Cells were washed and fixed, and the fluorescence ratiometric image (green/red) was taken with a confocal microscope.

soluble SNAP-tag protein and (N) SNAP-EGFR and can be optimized in future studies. However, the speed of labeling was still fast enough to study cell-surface protein dynamics, which usually occurs in time scales of hours.[23] Similarly, membrane-permeable DRBGFL-DA could readily label cytosolic SNAP-tag protein, producing a rapid and substantial rise in cytosolic fluorescence (Figure 3c). Thus, our FAPL probes should be applicable to a wide range of target proteins regardless of their location, i.e., either inside or outside of cells. In both cases, protein visualization was achieved simply by incubating cells with probes, requiring no washout process.

We expected that the use of membrane-impermeable DRBG-488 to visualize protein labeling only on the cell surface would allow us to design a system to visualize protein translocation across the cell membrane, such as endocytosis or exocytosis (Figure 4a).[25] These cellular events are important to control surface concentrations of receptors and to mediate cellular responses to physiological ligands.[24] Since these events occur dynamically, a real-time protein imaging system should be highly informative. In the continued presence of the FAPL probe, surface proteins would be continuously labeled and protein internalization would be measurable as a net increase of fluorescent vesicles inside cells (Figure 4b). To test this idea, we prepared SNAP-EGFR-CFP, in which both a SNAP-tag and a fluorescent protein are attached to the EGF receptor. In FAPL-based imaging, a signal was observed only on the plasma membrane before EGF stimulation, so internalization of endocytosed vesicles after EGF stimulation could be directly visualized and easily quantitated.[22] The image was much clearer than that of fluorescent protein (FP)-based imaging, since there was no contaminating signal from pre-existing internal proteins awaiting delivery to the cell surface (Figure 4c and Supplementary Movie 2 in the Supporting Information).

Next, we took advantage of the unique features of the FAPL method to study EGF receptor dynamics during EGF-induced

dx.doi.org/10.1021/ja200225m |J. Am. Chem. Soc. 2011, 133, 6745–6751

cell migration. It is known that derangement of endocytosis of certain receptors results in impaired migration, which strongly suggests the importance of controlled endocytosis for proper cell migration.[25,26] Several reports have suggested that EGF receptor distribution is polarized toward the leading edge after the onset of migration,[24,27] but it has been unclear how such a gradient could be maintained. We found that, as cells began to migrate upon EGF stimulation, a dramatic increase of vesicular internalization of the receptors was observed and newly formed vesicles were found in significantly greater numbers at the rear than at the front with respect to the migration direction ($P < 0.05$, ANOVA) (Figure 5 and Supplementary Movie 3 in the Supporting Information). This implies that endocytosis of the EGF receptor in stimulated cells may be slowed down at the leading edge as compared to the rear, and this would help maintain an increased surface distribution of EGF receptor at the leading edge. Alternatively, facilitated endocytosis of integrins and related proteins associated with Rho signaling at the rear of cells have been reported,[28,29] and a similar mechanism may govern the polarized sorting of EGF receptor during directional migration.

Finally, we demonstrated that the FAPL labeling system is also applicable to study exocytosis, namely, the surface delivery of newly synthesized proteins. Together with endocytosis, exocytosis of membrane proteins is an important process to maintain cell surface protein levels.[29,30] To distinguish newly plasma membrane-inserted proteins from pre-existing ones, pulse-chase labeling, where new and old proteins are labeled with different dyes, is classically performed.[11] However, because dye washout is essential, conventional pulse-chase labeling can only measure the total amount of secreted proteins accumulated during a labeling period on the scale of 1 h. In contrast, the FAPL method, which does not require washout, can in principle enable us to monitor changes of secreted protein in real time (Figure 6a). Indeed, optimization of pulse-chase labeling conditions allowed us to observe a time-dependent increase in chase fluorescence (DRBG-488), in contrast to the constant pulse fluorescence (BG-Alexa546) (Figure 6b,c and Supplementary Movie 4 in the Supporting Information). This increase was completely blocked by ATP starvation and partly inhibited by addition of protein synthesis inhibitors, such as cycloheximide, anisomycin, and rapamycin (Figure 6d), thus confirming that a substantial proportion of the live-imaged surface-delivery events consisted of insertion of newly synthesized (N) SNAP-EGFR into the plasma membrane. The fact that protein synthesis inhibitors did not completely block the fluorescence increase might arise from the presence of fast (protein-synthesis-independent) recycling loops of EGF receptor, which are likely to contribute to the observed changes in cell surface protein levels as well.[23]

Mis-translocation of EGF receptors is often observed in diseases showing uncontrollable cell growth, such as polycystic kidney disease (PKD) or multiple tumors,[31] so the study of EGF receptor surface-display mechanisms and the screening-based development of potential regulatory molecules will be helpful to investigate the pathogenesis and treatment of these diseases. The ease of use of our labeling method should make it an invaluable tool for these purposes, and studies along these lines are under way.

CONCLUSION

From the time that researchers first developed GFP as a biological research tool, visualization of protein movement has been growing to a powerful technique for analysis of protein functions.[1] Recently, small molecule-based protein labeling technique has also proved useful in the study, while one shortcoming was the requirement of washout of excess probes, a step that has precluded continuous monitoring of protein trafficking processes with all previously available probes.

To overcome the problem, we have designed and synthesized new protein labeling probes, which exhibit a strikingly large fluorescence activation coupled to the labeling reaction, and we thus obviated the need for any washout step in protein dynamics study. The key advantages of our method are the almost complete quenching of fluorescence in the unreacted probe molecules and the fast and highly selective labeling reaction with a tag-protein that can be generally used in a wide variety of experimental platforms. Indeed, the method enabled us to study the removal and insertion of cell surface receptors as real-time events and enabled us to understand the spatiotemporal dynamics of EGF receptor endocytosis during cell migration. Further, because our FAPL method can be applied to any target protein regardless of location inside or outside the cells, it should make feasible a variety of novel imaging techniques, such as superhigh-resolution imaging of target proteins inside living cells[32] and high-throughput screening or *in vivo* imaging[17] where washout is undesirable or impossible. The probe design can be easily adjusted as required by means of chemical modification, and thus, we believe this method represents a versatile tool to analyze dynamic protein behaviors in living systems.

ASSOCIATED CONTENT

Supporting Information. Structures of key compounds used in the study; experimental conditions; supplementary methods for chemical synthesis and characterization of compounds; Schemes S1−S3; supplementary experiments and data; Figures S1−S9; supplementary movies (Supplementary Movies 1−4; avi and mpg files); supplementary references; and personal acknowledgement. This material is available free of charge via the Internet at http://pubs.acs.org.

AUTHOR INFORMATION

Corresponding Author
uranokun@m.u-tokyo.ac.jp

ACKNOWLEDGMENT

We thank Yayoi Kondo for technical support in DNA and cellular experiments and Dr. Masanori Osawa for technical support in soluble protein preparation. We also thank W. R. S. Steele for careful proofreading of the paper. This work was financially supported by the Ministry of Education, Culture, Sports, Science and Technology of Japan (Grant Nos. 20117003 and 19205021 to Y.U., and Specially Promoted Research 22000006 to T.N. and a Global COE Program "Center of Education and Research for Chemical Biology of the Diseases"). T.N. was also supported by the Hoh-ansha Foundation. T.K. was a recipient of a fellowship from Japanese Society for the Promotion of Science.

REFERENCES

(1) Tsien, R. Y. *Nat. Rev. Mol. Cell. Biol.* **2003**, No. Suppl, SS16–21.
(2) Griffin, B. A.; Adams, S. R.; Tsien, R. Y. *Science* **1998**, *281*, 269–272.

(3) Johnsson, K. *Nat. Chem. Biol.* **2009**, *5*, 63–65.
(4) Chen, I.; Ting, A. Y. *Curr. Opin. Biotechnol.* **2005**, *16*, 35–40.
(5) Fernandez-Suarez, M.; Baruah, H.; Martínez-Hernández., L.; Xie, K. T.; Baskin, J. M.; Bertozzi, C. R.; Ting, A. Y. *Nat. Biotechnol.* **2007**, *25*, 1483–1487.
(6) Keppler, A.; Gendreizig, S.; Gronemeyer, T.; Pick, H.; Vogel, H.; Johnsson, K. *Nat. Biotechnol.* **2003**, *21*, 86–89.
(7) Tour, O.; Adams, S. R.; Kerr, R. A.; Meijer, R. M.; Sejnowski, T. J.; Tsien, R. W.; Tsien, R. Y. *Nat. Chem. Biol.* **2007**, *3*, 424–431.
(8) Marek, K. W.; Davis, G. W. *Neuron* **2002**, *36*, 805–813.
(9) Maurel, D.; Banala, S.; Laroche, T.; Johnsson, K. *ACS Chem. Biol.* **2010**, *5*, 507–516.
(10) Vivero-Pol, L.; George, N.; Krumm, H.; Johnsson, K.; Johnsson, N. *J. Am. Chem. Soc.* **2005**, *127*, 12770–12771.
(11) Jacquier, V.; Prummer, M.; Segura, J.-M.; Pick, H.; Vogel, H. *Proc. Natl. Acad. Sci. U.S.A.* **2006**, *103*, 14325–14330.
(12) Gaietta, G.; Deerinck, T. J.; Adams, S. R.; Bouwer, J.; Tour, O.; Laird, D. W.; Sosinsky, G. E.; Tsien, R. Y.; Ellisman, M. H. *Science* **2002**, *296*, 503–507.
(13) Komatsu, T.; Kikuchi, K.; Takakusa, H.; Hanaoka, K.; Ueno, T.; Kamiya, M.; Urano, Y.; Nagano, T. *J. Am. Chem. Soc.* **2006**, *128*, 15946–15947.
(14) Mizukami, S.; Watanabe, S.; Hori, Y.; Kikuchi, K. *J. Am. Chem. Soc.* **2009**, *131*, 5016–5017.
(15) Stöhr, K.; Siegberg, D.; Ehrhard, T.; Lymperopoulos, K.; Öz, S.; Schulmeister, S.; Pfeifer, A. C.; Bachmann, J.; Klingmüller, U.; Sourjik, V.; Herten, D.-P. *Anal. Chem.* **2010**, *82*, 8186–8193.
(16) Zlokarnik, G.; Negulescu, P. A.; Knapp, T. E.; Mere, L.; Burres, N.; Feng, L.; Whitney, M.; Roemer, K.; Tsien, R. Y. *Science* **1998**, *279*, 84–88.
(17) Blum, G.; Mullins, S. R.; Keren, K.; Fonovic, M.; Jedeszko, C.; Rice, M. J.; Sloane, B. F.; Bogyo, M. *Nat. Chem. Biol.* **2005**, *1*, 203–209.
(18) Wibley, J. E.; Pegg, A. E.; Moody, P. C. *Nucleic Acids Res.* **2000**, *28*, 393–401.
(19) Gautier, A.; Juillerat, A.; Heinis, C.; Reis Correa, I., Jr.; Kindermann, M.; Beaufils, F.; Johnsson, K. *Chem. Biol.* **2008**, *15*, 128–136.
(20) Carter, R. E.; Sorkin, A. *J. Biol. Chem.* **1998**, *273*, 35000–35007.
(21) Hackel, P. O.; Zwick, E.; Prenzel, N.; Ullrich, A. *Curr. Opin. Cell Biol.* **1999**, *11*, 184–189.
(22) Hynes, N. E.; Lane, H. A. *Nat. Rev. Cancer* **2005**, *5*, 341–354.
(23) Vieira, A. V.; Lamaze, C.; Schmid, S. L. *Science* **1996**, *274*, 2086–2089.
(24) Chung, I.; Akita, R.; Vandlen, R.; Toomre, D.; Schlessinger, J.; Mellman, I. *Nature* **2010**, *464*, 783–788.
(25) Mosesson, Y.; Mills, G. B.; Yarden, Y. *Nat. Rev. Cancer* **2008**, *8*, 835–850.
(26) Sorkin, A.; Von Zastrow, M. *Nat. Rev. Mol. Cell Biol.* **2002**, *3*, 600–614.
(27) Ouyang, M.; Lu, S.; Li, X. Y.; Xu, J.; Seong, J.; Giepmans, B. N.; Shyy, J. Y.; Weiss, S. J.; Wang, Y. *J. Biol. Chem.* **2008**, *283*, 17740–17748.
(28) Caswell, P.; Norman, J. *Trends Cell Biol.* **2008**, *18*, 257–263.
(29) Schlunck, G.; Damke, T.; Kiosses, W. B.; Rusk, N.; Symons, M. H.; Waterman-Storer, C. M.; Schmid, S. L.; Schwartz, M. A. *Mol. Biol. Cell* **2004**, *15*, 256–267.
(30) Radisky, D. C.; Stallings-Mann, M.; Hirai, Y.; Bissell, M. J. *Nat. Rev. Mol. Cell Biol.* **2009**, *10*, 228–234.
(31) Hobert, M. E.; Kil, S. J. M.; Medof, M. E.; Carlin, C. R. *J. Biol. Chem.* **1997**, *272*, 32901–32909.
(32) Hell, S. W.; Schmidt, R.; Egner, A. *Nat. Photonics* **2009**, *3*, 381–387.